Synthetic Metals 203 (2015) 208–214

Contents lists available at ScienceDirect

Synthetic Metals

journal homepage: www.elsevier.com/locate/synmet

Viability of stretchable poly(3-heptylthiophene) (P3HpT) for organic solar cells and field-effect transistors

Suchol Savagatrup [a,1], Adam D. Printz [a,1], Haosheng Wu [b], Kirtana M. Rajan [a], Eric J. Sawyer [a], Aliaksandr V. Zaretski [a], Christopher J. Bettinger [b], Darren J. Lipomi [a,*]

[a] Department of NanoEngineering, University of California, San Diego, 9500 Gilman Drive Mail Code 0448, La Jolla, CA 92093-0448, USA
[b] Department of Materials Science and Engineering, Carnegie Mellon University, 5000 Forbes Avenue, Pittsburgh, PA 15213-3890, USA

ARTICLE INFO

Article history:
Received 25 January 2015
Received in revised form 18 February 2015
Accepted 21 February 2015
Available online xxx

Keywords:
Mechanical properties
Organic solar cells
Poly(3-alkylthiophene)
Stretchable electronics
P3HpT

ABSTRACT

Mechanical compliance is a critical attribute for organic semiconductors in flexible, stretchable, mechanically robust, and biologically integrated electronics. This paper substantially develops the observation that a small change in the length of the alkyl side chain of regioregular poly(3-alkylthiophene)s has a dramatic effect on the interplay between their mechanical and charge-transport properties. Specifically, the thermal, mechanical, and charge-transport properties of poly(3-heptylthiophene) (P3HpT, $n=7$), which we found to be an unusual example of a stretchable semiconducting thermoplastic, are described in comparison to those of poly(3-hexylthiophene) (P3HT, $n=6$) and poly(3-octylthiophene) (P3OT, $n=8$). Neat P3HpT was found to have mechanical properties similar to that of P3OT, and when mixed in 1:1 blends with the fullerene [6,6]-phenyl C_{61} butyric acid methyl ester (PCBM), exhibited electronic properties comparable to P3HT. However, the charge-carrier mobility of neat P3HpT is substantially inferior to that of P3HT; the good performance of P3HpT-based solar cells is the result of improved mobility in P3HpT:PCBM blends compared to the neat material. While P3HpT may be a favorable alternative to P3HT in ultra-flexible, stretchable, and mechanically robust organic solar cells, P3HpT would only make a good field-effect transistor in situations in which mechanical compliance was more important than high mobility.

© 2015 Elsevier B.V. All rights reserved.

1. Introduction

Given the vast literature devoted to the regioregular poly(3-alkylthiophene)s (P3ATs), it may seem that every aspect of the chemical, physical, and optoelectronic properties of this class of materials have been characterized exhaustively. This paper shows that a small change in the length of the alkyl side chain—in the range of $6 \leq n \leq 8$—nevertheless has profound effects on these properties, in particular the flexibility, stretchability, and resistance to mechanical failure of devices. The mechanical properties of organic semiconductors are highly variable and sensitive to small molecular and microstructural changes [1–4]. Moreover, there is substantial evidence that suggests that good charge-transport and mechanical compliance are mutually exclusive properties [5,6]. We recently reported the tensile moduli of a series of P3AT homopolymers and copolymers and their power conversion efficiencies (*PCEs*) when combined in 1:1 blends with [6,6]-phenyl C_{61} butyric acid methyl ester (PCBM) in organic solar cells (OSCs) [2]. We found that the tensile moduli of the thin films (E_f) exhibited a drop-off of more than one order of magnitude when the length of the side chain was increased from six carbon atoms—as in poly(3-hexylthiophene) (P3HT, $E_f = 1.0$ GPa) the workhorse of organic electronics—to seven carbon atoms, as in poly(3-heptylthiophene) (P3HpT, $E_f = 0.07$ GPa) [2]. Spectroscopic evidence using the weakly interacting H-aggregate model showed similarities in the level of order between P3HT and P3HpT, and both materials exhibited similar photovoltaic performance. The good performance of P3HpT, especially in the context of OSCs, suggested to us that P3HpT could be useful in applications that demand mechanical flexibility, stretchability, and robustness (that is, some applications of organic semiconductors that currently use P3HT). The purpose of this paper is to develop substantially our previous finding by characterizing the thermal, mechanical, photovoltaic, and charge-transport properties of P3HpT in comparison to P3HT and poly(3-octylthiophene) (P3OT) for pure films (i.e., for thin-film transistors) and when blended with PCBM (i.e., for solar cells, Fig. 1a). Our measurements point to seemingly minor changes in the chemical structure of polymers that can have

* Corresponding author. Tel.: +1 858 246 1227.
E-mail address: dlipomi@eng.ucsd.edu (D.J. Lipomi).
[1] Equal contribution.

http://dx.doi.org/10.1016/j.synthmet.2015.02.031
0379-6779/© 2015 Elsevier B.V. All rights reserved.

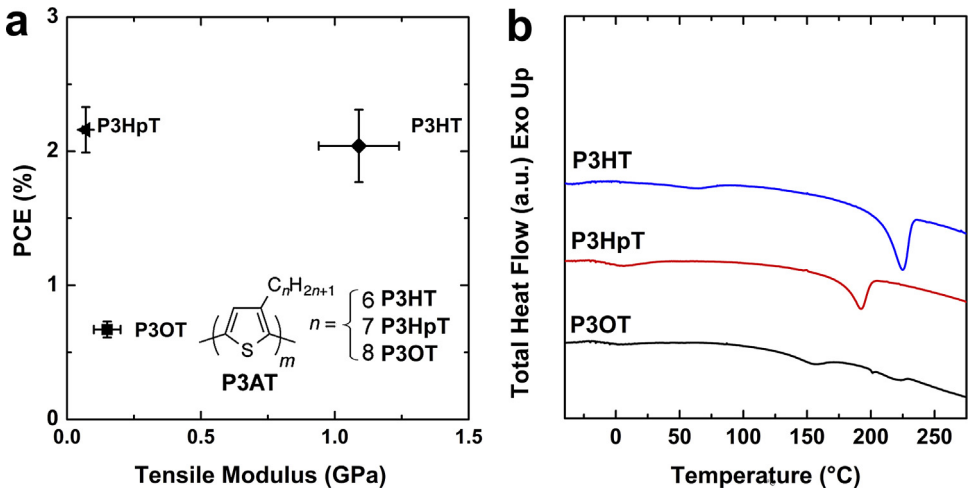

Fig. 1. (a) Plot of power conversion efficiency of the P3ATs in a 1:1 blend with $PC_{61}BM$ vs. tensile moduli of the pure polymers. The position of P3HpT well above and to the left of the line connecting P3HT and P3OT suggests the possibility of co-optimization of photovoltaic and mechanical properties (data reproduced from Ref. [2]). (b) DSC thermograms of representative P3HT, P3HpT, and P3OT samples at a heating rate of 10 °C min^{-1}. The chemical structures are inset in the figure. T_g values of 11 to 13 °C were determined for P3HT, −5 to −4 °C for P3HpT, and −10 to −8 °C for P3OT. T_m values were observed at 225, 192, and 155 °C for P3HT, P3HpT, and P3OT, respectively. (For interpretation of the references to color in text, the reader is referred to the web version of this article.)

dramatic effects on their physical properties. We found that P3HpT is in fact an unusual example of a stretchable semiconducting thermoplastic. While we believe P3HpT is an excellent candidate to replace P3HT in OSCs, its high mobility in this context seems to be the result of blending with fullerenes. In pure form, as required for organic thin-film transistors, the material is more elastic and ductile than P3HT, but the charge-carrier mobility of P3HpT is inferior to that of P3HT.

2. Results and discussion

2.1. Characterization of the polymers

P3HT, P3HpT, and P3OT were examined for regioregularity and purity using ^1H NMR spectra. The percent regioregularity for each sample was as follows: P3HT, 88%; P3HpT, 92%; and P3OT, 82%. We observed no additional peaks beside those expected (Fig. S1, Supporting information). From size-exclusion chromatography, we determined that the molecular weights of the polymers are as follows: P3HT, M_n = 44 kDa, PDI = 2.0; P3HpT, M_n = 35 kDa, PDI = 1.5; and P3OT, M_n = 34 kDa, PDI = 2.5.

2.2. Thermal properties

The intuitive rationale for the increase in elasticity and ductility measured as a function of increasing length of the side chain P3AT (a comb-like polymer) is a reduction in the density of load-bearing carbon–carbon bonds along the main chain per cross sectional area [1,7]. The glass transition temperature (T_g) for comb-like polymers also decreases with increasing length of the side chain until a critical value, after which T_g remains roughly constant or even increases [8]. Long side chains installed for solubility on otherwise rigid backbone structures thus have deleterious consequences for polymers intended for structural applications [9]. For flexible and stretchable organic devices, however, high compliance (low tensile modulus) is desirable. Values of T_g in the literature occupy a wide range of values for P3HT, but it seems that the consensus value is equal to or slightly less than room temperature (i.e., 15–25 °C, though our experience is that research laboratories are often kept at temperatures significantly below 25 °C) [5]. The value for P3OT is unequivocally below room temperature [10], and we have used the ductility of P3OT:PCBM composites at ambient temperature to stretch, conform, and bond whole OSCs to hemispherical surfaces without generating cracks or wrinkles [11].

We used differential scanning calorimetry (DSC, Fig. 1b) to measure the T_g and melting temperature (T_m) of P3HpT (red curve) and compared it to those of P3HT (blue curve) and P3OT (black curve). From the analysis of the total heat flow for the heating of the pure polymer samples, we found values of T_g between 11 and 13 °C for P3HT, −5 and −4 °C for P3HpT, and −10 and −8 °C for P3OT. These data are consistent with decreasing T_g with increasing length of the side chain, and that T_g is substantially below room temperature for P3HpT and P3OT. The melting temperatures, T_m, also decreased with increasing length of the side chain, which agreed with previously reported results [12]. We note that the values of T_g found in literature can vary significantly due to the different heating rates employed and the thermal history of the sample. The relationship of T_g for P3HpT and P3OT to ambient temperature suggests that these materials can be treated as stretchable semiconducting thermoplastics. Our experience with OSCs based on either P3HpT or P3OT, however, suggests that the two polymers have significantly different semiconducting performance.

The addition of fullerene to P3HT has previously been reported to produce a greater T_g in the blend compared to that of the neat polymer [13]. We reasoned that this increase in T_g would occur in all P3ATs, and that the good photovoltaic performance of P3HpT:PCBM might be produced concomitantly with anti-plasticization of P3HpT by PCBM. To determine if the T_g of the P3ATs increased significantly with the addition of PCBM, we analysed the total heat flow for the P3AT:PCBM samples. We found the T_g of P3HT:PCBM increased to the range between 37 and 40 °C, which agrees with previously reported results [14], and the T_g of P3OT:PCBM increased to the range between −5 and 0 °C. Interestingly, the T_g of P3HpT:PCBM increased to the range between 33 and 35 °C, which is close to that of P3HT:PCBM. The similarity in T_g between P3HT:PCBM and P3HpT:PCBM is consistent with their similar photovoltaic properties [2].

2.3. Band structure

Increasing the length of the side chain in P3ATs has a very small effect on the bandgap, however, with a side chain longer than n = 6, the absolute positions of the frontier molecular orbitals decrease in

energy (become more negative relative to the vacuum level) [15]. To verify this trend previously identified in the literature for P3ATs with an even number of carbon atoms in the side chains [15], we measured the positions of the HOMOs for the three P3ATs by cyclic voltammetry. The onset of oxidation (E_{OX}) for P3HT, P3HpT, and P3OT can be seen in Fig. 2a, which reveals a linear dependence on ionization potential with the length of the side chain. To determine the LUMO, we added the optical band gap, $E_{g,opt}$, and 0.3 eV to the HOMO. The 0.3 eV is added because it is the typical difference between the optical and electrochemical band gaps, previously attributed to the exciton binding energy [16]. The absorption spectra of the solid films, shown in Fig. 2b, reveal similar onsets of absorption, 1.92–1.94 eV (639–646 nm). The spectra also show better order in P3HT and P3HpT compared to P3OT. The optical and electrochemical properties of the P3ATs are summarized in Table 1. We initially hypothesized that similar order when $n = 6$ or 7 would produce similar charge-carrier mobilities, though the effect of unequal T_g between P3HT and P3HpT could also play a role.

Table 1
Optical and electrochemical properties of the P3ATs.

Material	E_{ox} (V)	HOMO(eV)[a]	$E_{g,opt}$ (eV)	LUMO (eV)[b]
P3HT	0.54	−5.25	1.94	−3.01
P3HpT	0.68	−5.39	1.92	−3.17
P3OT	0.75	−5.46	1.92	−3.24

[a] HOMO = $-e(E_{ox} + 4.71)$ eV.
[b] LUMO = $E_{g,opt} + 0.3 +$ HOMO eV.

2.4. Charge transport properties

The good charge-transport properties of P3ATs are generally attributed to the semicrystalline morphology in which well ordered aggregates (observed spectroscopically or by X-ray diffraction) have been correlated with high hole mobilities in organic thin-film transistors (OTFTs) and good efficiencies in OSCs [5,17]. To compare directly the field-effect hole mobility, μ_h, for P3HT, P3HpT, and P3OT, we fabricated bottom-gate, bottom-contact thin-film transistors with the dimensions of 500 μm (channel width) and 10 μm (channel length). Fig. 3a–c shows the output plots and Fig. 3d shows the transfer plots for P3HT, P3HpT, and P3OT. The field effect mobilities, μ_h, were extracted from the slopes of the linear fits in the saturation regime on the plots of $(-I_{DS})^{1/2}$ vs. V_{GS} (Fig. 3d), and the threshold voltages, V_T, were extracted from the interception of the linear fits and the x-axis using Eq. (1) [18,19],

$$\sqrt{I_{DS}} = \sqrt{\mu_h C_d \frac{W}{2L}}(V_{GS} - V_T) \quad (1)$$

where $C_d = 1.38 \times 10^{-8}$ F cm^{-2}, $W = 500$ μm, and $L = 10$ μm. The mobilities, threshold voltage, and on-off ratios extracted from the current–voltage characteristics for the three materials are listed in Table 2.

As expected, P3HT exhibited the greatest mobility, 0.01 cm^2 V^{-1} s^{-1}, while P3OT exhibited the lowest, 0.0001 cm^2 V^{-1} s^{-1}. The mobility of P3HpT was intermediate, 0.0006 cm^2 V^{-1} s^{-1}, but closer to that of P3OT than to that of P3HT. Although P3HT, P3HpT, and P3OT have different HOMO values (Table 1), the injection barriers at Au/P3AT interfaces are sufficiently small (work function of Au $\Phi_M \approx 5.1 \sim 5.3$ eV) [20,21] and should only result in minimal differences among three differenct P3AT samples in contact resistance values, which are largely dominated by the polymer nanomorphologies at the Au/channel contact edges in bottom-contact OTFT configuration [22]. The disparity in hole mobilities could be a manifestation of the thermal properties, where the amorphous domains are less mobile for P3HT than they are for P3HpT or P3OT. The relative rigidity of the amorphous domains of P3HT could be conducive to greater charge mobility than P3HpT, despite the similarity in aggregation apparent in the UV–vis spectra of the solid films (Fig. 2b).

The low hole mobility of P3HpT should be deleterious to photovoltaic performance, yet we found that P3HpT:PCBM devices performed as well as P3HT:PCBM devices [16]. It has been reported by others that blending MDMO-PPV with PCBM can improve the hole mobility of the polymer by orders of magnitude [23,24]. The exact mechanism that produces the improvement in mobility is unknown, but it has been speculated that the presence of the fullerene improves ordering in the polymer [25]. We therefore tested this hypothesis for the three P3AT:PCBM composites. The hole mobility of P3HT, 0.01 cm^2 V^{-1} s^{-1}, remained similar to that of the neat polymer, however, the mobilities of P3HpT and P3OT increased by an order of magnitude to 0.004 cm^2 V^{-1} s^{-1} and 0.001 cm^2 V^{-1} s^{-1}, respectively. Such a large increase in μ_h for P3HpT and P3OT with the addition of fullerene correlates with the increase in T_g. These results support the hypothesis that immobilization of polymer chains with the incorporation of an

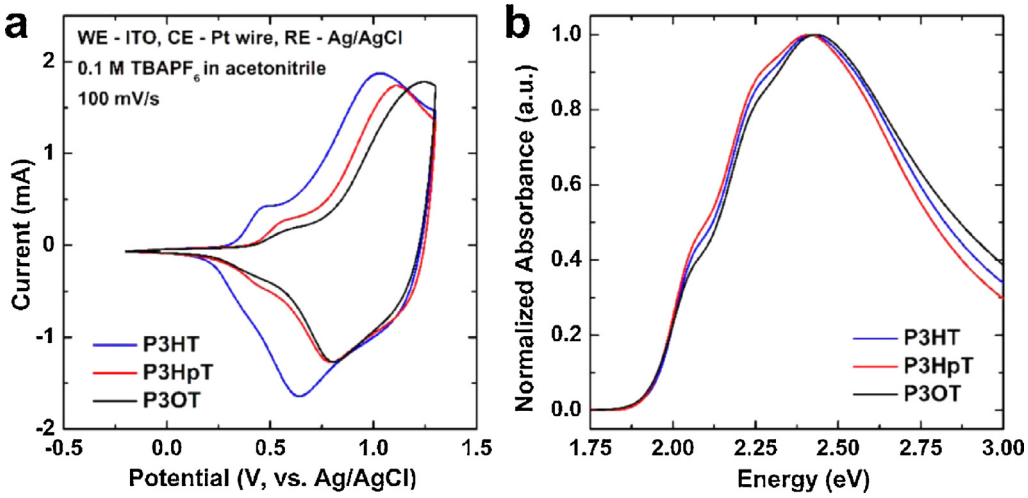

Fig. 2. Determination of the HOMO and LUMO for P3HT, P3HpT, and P3OT. (a) Cyclic voltammetry oxidation curves measured at a scan rate of 100 mV s^{-1}. (b) Absorption spectra of the polymer thin films on ITO and annealed at 100 °C for 30 min.

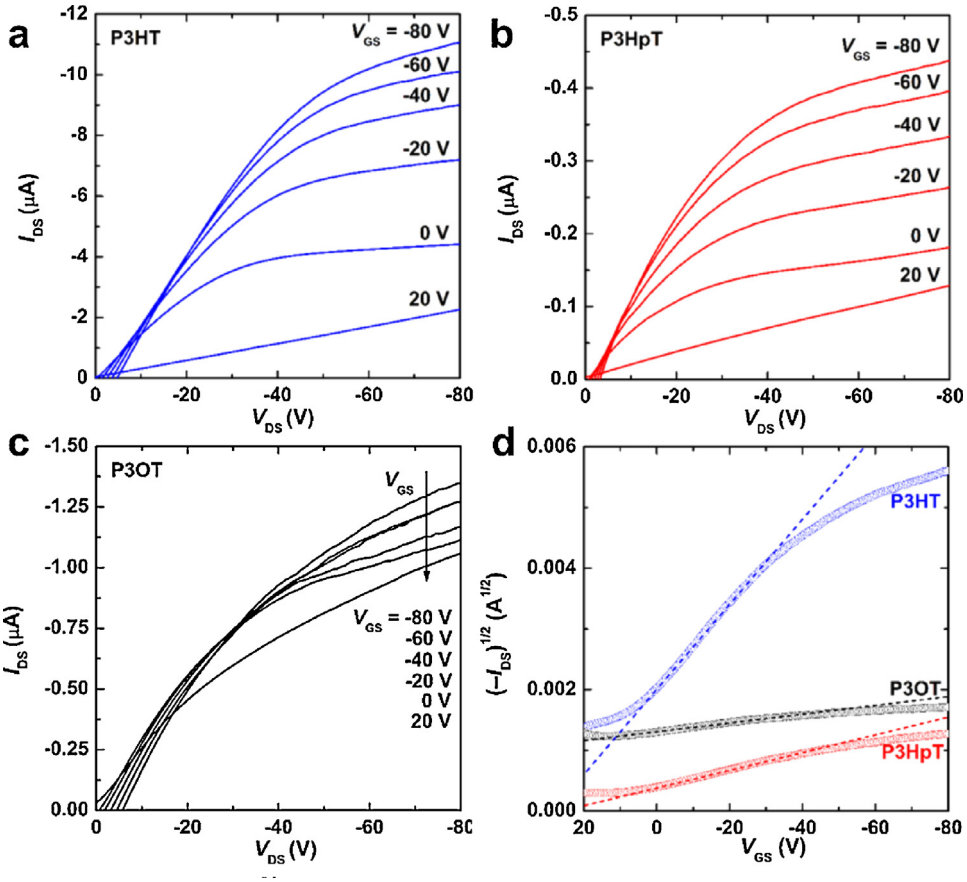

Fig. 3. Electrical characteristics of P3AT organic thin films transistors (OTFTs): current–voltage output characteristics of a 10 μm (length) by 500 μm (width) channel for (a) P3HT, (b) P3HpT, and (c) P3OT. (d) Transfer characteristics $(-I_{DS})^{1/2}$ vs. V_{GS} at V_{DS} = −80 V with respect to alkyl side chain length. Dashed lines represent the linear fit in the saturation regime.

anti-plasticizer may increase the mobility and thus the photovoltaic performance.

2.5. Combined mechanical and photovoltaic properties

Given that the charge-transport properties of P3HpT compare favorably to those of P3HT, we believed that P3HpT might be useful as a stretchable and mechanically robust semiconductor for flexible solar cells and wearable devices. Fig. 4a compares the representative *J–V* curves of the three P3AT:PCBM devices and the figures of merit are summarized in Table 3. P3HT:PCBM and P3HpT:PCBM exhibited similar power conversion efficiencies, while P3OT:PCBM performed considerably poorer.

The necessity to add fullerenes (e.g., PCBM) to conjugated polymers to make a bulk heterojunction has the unwanted effect of increasing the stiffness and brittleness of the composite film [1,2,26]. We hypothesized that there may be a concentration of PCBM that maximized both compliance and power conversion efficiency (*PCE*) of solar cells with the architecture glass/PEDOT:PSS/P3HpT:PCBM/eutectic gallium–indium (EGaIn). Fig. 4b plots the *PCE* of P3HpT:PCBM blend as a function of the weight fraction of PCBM in the blend. The tensile modulus (E_f, left vertical axis) and the crack-onset strain (*CoS*, right vertical axis) as a function of PCBM concentration are plotted in Fig. 4c. We observed that the three quantities were highly correlated. This apparent trade-off between stiffness and electronic performance has been observed before in polythiophenes exhibiting different levels of crystalline order, specifically P3HT:PCBM blends with different order in the polymer phase produced by different rates of drying during solution casting [5], and in the conductive polyelectrolyte complex PEDOT:PSS, when spin-coated from inks containing different concentrations of dimethylsulfoxide (DMSO) [27].

We also examined the effect of PCBM concentration on the extent of ordering in the polymer component, as measured by UV–vis spectroscopy and analysed by the weakly interacting H-aggregate model (Fig. 4d). The UV–vis spectra can be deconvoluted into contributions from the aggregated material (the lower-energy shoulders in the spectra) and from the amorphous material. The

Table 2
Average mobility values obtained from the transfer curve of the P3HT, P3HpT, and P3OT OTFTs.

Materials	Mobility, μ_h($\times 10^{-3}$)(cm^2/V s)	Threshold voltage, V_T (V)	On-off ratio[a]
P3HT	11 ± 1.8	34.5 ± 3.63	13.8 ± 3.00
P3HpT	0.55 ± 0.082	36.4 ± 4.25	10.2 ± 2.44
P3OT	0.14 ± 0.032	180 ± 32.0	1.68 ± 0.21
P3HT:PCBM	10 ± 3.3	12.8 ± 5.63	375 ± 231
P3HpT:PCBM	4.0 ± 1.0	23.5 ± 4.47	165 ± 86.8
P3OT:PCBM	1.2 ± 0.66	45.0 ± 18.1	48.8 ± 33.2

[a] On-off ratios were calculated through $I(V_{GS}$ = −80 V)/$I(V_{GS}$ = +20 V).

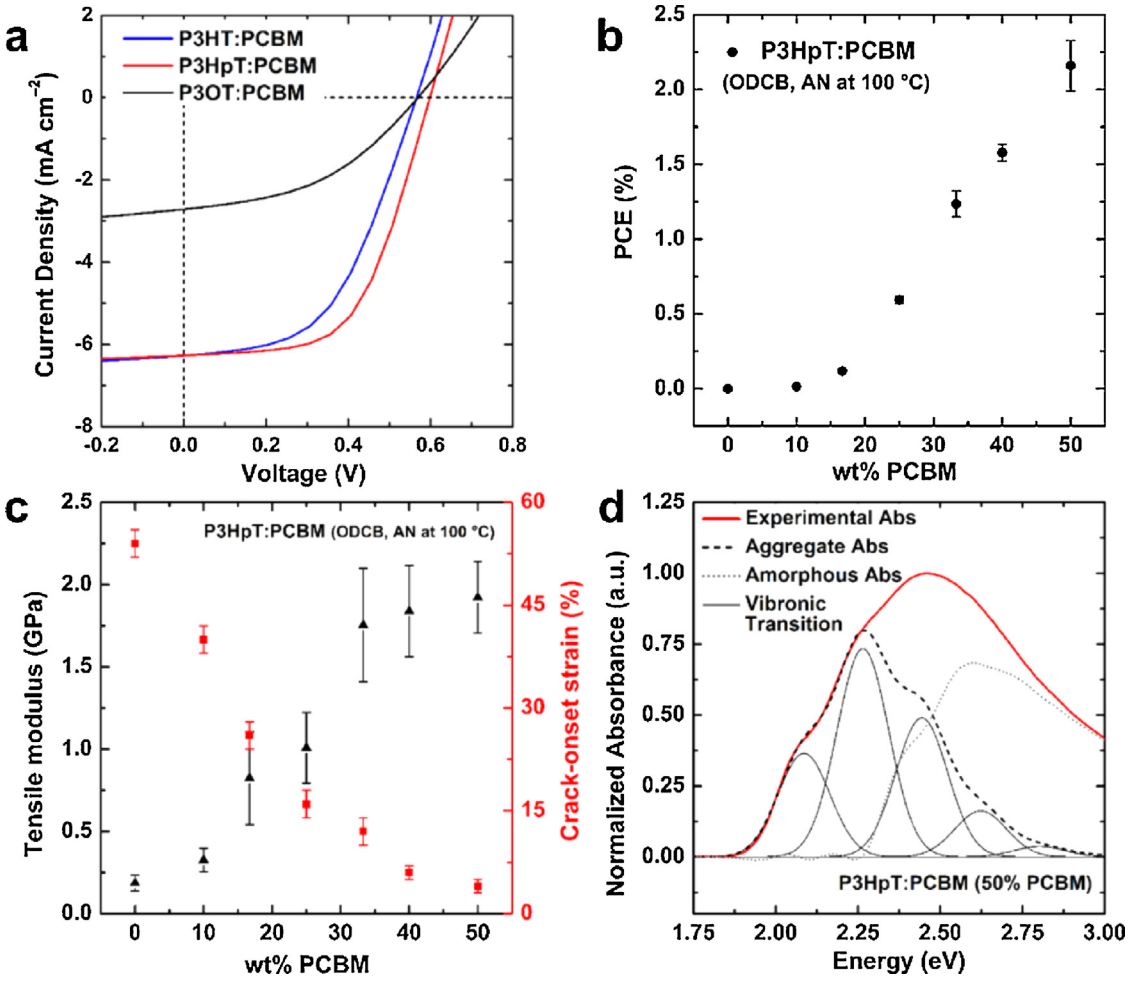

Fig. 4. (a) *J–V* curves of average devices ($N \geq 7$) with an active layer of 1:1 blend of P3AT and $PC_{61}BM$. The architecture of the devices was PEDOT:PSS/P3AT:PCBM/EGaIn. The data were reproduced from Ref. [2]. (b) Power conversion efficiency of average devices ($N \geq 7$) comprising P3HpT and PCBM as a function of weight fraction of PCBM. (c) Values of tensile modulus and crack-onset strain of P3HpT:PCBM as a function of weight fraction of PCBM. All films were fabricated by spin-coating from solutions of ODCB and thermally annealed at 100 °C. (d) Example of deconvolution of the absorption spectra into vibronic transitions of ordered P3HpT and amorphous absorption using the weakly interacting H-aggregate model.

percent aggregate has been correlated to increased stiffness and crack-onset strain in P3HT:PCBM blends [5]. Interestingly, small concentrations of PCBM appear to have an ordering effect on the polymer, however this effect disappears with larger loading of PCBM. Both the *W* value, which is inversely related to the aggregate order, and the aggregate fraction suggests that a decrease in ordering begins with a loading of PCBM above 33.3%. At lower loadings, the PCBM is likely to be dispersed in the amorphous domains of the polymer [28]; at higher loadings, larger PCBM-rich domains form that serve as electron-conducting regions required for efficient solar cells, but are also hard inclusions in the film that stiffen and embrittle the film and are deleterious to polymer ordering. Of note, these results suggest that the increase in hole mobility we measured in 1:1 P3AT:PCBM blends is not due to increased polymer ordering, and thus, further studies are required to fully understand the mechanism responsible.

We note that molecular weight affects the mechanical properties of the P3ATs in ways that have not yet been fully characterized. For example, Bruner and Dauskardt found that cohesive fracture energy of P3HT increases with molecular weight (M_w) in a range of 28–100 kDa [29], while the entanglement molecular weight has been estimated to be 10–20 kDa for P3HT [28]. Koch et al. observed that monodisperse samples of P3HT with exceptionally low degrees of polymerization (dp = 12) can exhibit structures in which the side chains intercalate that have been described qualitatively as brittle [30]. We have previously found that the tensile modulus was similar within experimental error for

Table 3
Characteristics of P3HpT:PCBM films as a function of weight percentage of PCBM. All films were spin-coated from ODCB and thermally annealed at 100 °C.

Wt% PCBM[a]	*PCE* (%)[b]	E_f (GPa)[c]	*CoS*(%)[d]	*W* (eV)[e]	Agg. fraction[f]
0%	–	0.19 ± 0.05	54 ± 2	0.181	0.547
10%	0.014 ± 0.002	0.33 ± 0.07	40 ± 2	0.165	0.552
16.7%	0.12 ± 0.01	0.82 ± 0.28	26 ± 2	0.168	0.555
25%	0.59 ± 0.03	1.01 ± 0.22	16 ± 2	0.169	0.550
33.3%	1.24 ± 0.09	1.75 ± 0.35	12 ± 2	0.169	0.547
40%	1.58 ± 0.06	1.84 ± 0.28	6 ± 1	0.172	0.518
50%	2.16 ± 0.17	1.92 ± 0.22	4 ± 1	0.179	0.464

[a] The weight percentage of PCBM in the solution prepared in ODCB.
[b] The architecture of the OSC devices was PEDOT:PSS/P3HpT:PCBM/EGain. The thickness of the active layer for each sample was ~150 nm. The power conversion efficiencies were averages of $N \geq 8$ devices.
[c] Tensile modulus of each sample was determined by the buckling-based methodology.
[d] Crack-onset strain was determined by transferring the film of each sample (~150 nm) onto an unstrained PDMS substrate and incrementally increasing the induced strain. Optical micrographs were taken to observe the formation of cracks.
[e] The exciton bandwidth, *W*, which is inversely correlated to aggregate order.
[f] The aggregate fraction were calculated from a least-squares fit of the weakly interacting H-aggregate model to the absorption spectra.

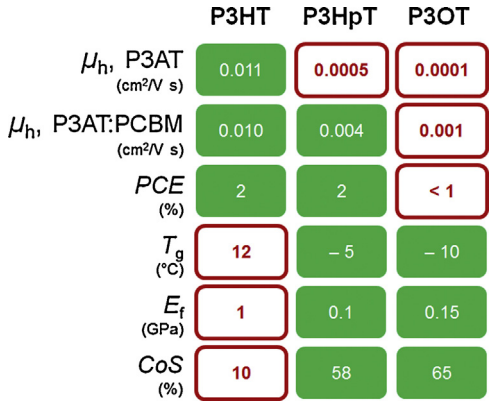

Fig. 5. A summary of the electronic and mechanical properties of the polymers and polymer:fullerene blends studied in this work. Favorable properties are highlighted in green (closed boxes), while unfavorable properties are highlighted in red (open boxes). (For interpretation of the references to color in this figure legend, the reader is referred to the web version of this article.)

P3HT with M_n between 7 and 44 kDa [2,11]. We thus did not attribute differences in mechanical properties to differences in the molecular weight (M_n) of the samples used in this study (P3HT 44 kDa, P3HpT 35 kDa, P3OT 34 kDa).

A summary of the electronic and mechanical properties of P3HT, P3HpT, and P3OT is presented in Fig. 5. While P3HT has a favorable μ_h and *PCE*, it exhibits poor compliance and ductility. P3OT, on the other hand, has high compliance and ductility, but poor μ_h and *PCE*. In contrast, P3HpT is a chimera; in neat films, it has a similar compliance and ductility to P3OT, and when blended with fullerene, its electronic performance becomes closer to or equal to that of P3HT. While P3HpT is stiffened by PCBM, the blend is still less stiff than P3HT:PCBM by a factor of approximately two: $E_f = 1.46 \pm 0.16$ GPa for P3HpT:PCBM compared to 2.75 ± 0.59 GPa for P3HT:PCBM [31].

3. Conclusions

Poly(3-heptylthiophene) is an interesting example of a semiconducting thermoplastic elastomer (STE). While P3OT could also be described as an STE, the semiconducting performance of P3HpT is better, especially when blended with PCBM. The mechanical compliance of P3HpT arises from the fact that its glass transition is the first in the series of P3ATs that is well below ambient temperature. When compared to P3HT and P3OT, the *PCE* of an organic solar cell with an active layer comprising P3HpT:PCBM is comparable to that of P3HT:PCBM, while the hole mobility of P3HpT is poor—closer to P3OT than P3HT—it is increased by nearly an order of magnitude with the addition of PCBM. P3HpT is thus attractive as a potential replacement for P3HT in flexible, stretchable, wearable, and mechanically robust solar cells, though it would not make an especially good transistor. More generally, the behavior observed in these relatively simple conjugated polymer systems should provide insight into designing highly elastic and high performing organic electronic devices in outdoor, portable, and wearable applications that require mechanical robustness.

Notes

Electronic Supplementary information (ESI) available: experimental methods, UV–vis absorption spectra for P3HpT:PCBM at different concentrations, DSC of the P3AT:PCBMs, method for determining E_{ox} from CV, and charge transport of P3AT:PCBMs.

Acknowledgments

This work was supported by the Air Force Office of Scientific Research (AFOSR) Young Investigator Program, grant number FA9550-13-1-0156. Additional support was provided by the National Science Foundation Graduate Research Fellowship, awarded to both S. Savagatrup and A.V. Zaretski, and by laboratory startup funds from the University of California, San Diego. The authors thank Prof. J. Wang and A. Bandodkar for helpful discussions and use of their equipment to perform cyclic voltammetry experiments.

Appendix A. Supplementary data

Supplementary data associated with this article can be found, in the online version, at http://dx.doi.org/10.1016/j.synthmet.2015.02.031.

References

[1] S. Savagatrup, A.S. Makaram, D.J. Burke, D.J. Lipomi, Mechanical properties of conjugated polymers and polymer–fullerene composites as a function of molecular structure, Adv. Funct. Mater. 24 (2014) 1169, doi:http://dx.doi.org/10.1002/adfm.201302646.
[2] S. Savagatrup, A.D. Printz, D. Rodriquez, D.J. Lipomi, Best of both worlds: conjugated polymers exhibiting good photovoltaic behavior and high tensile elasticity, Macromolecules 47 (2014) 1981, doi:http://dx.doi.org/10.1021/ma500286d.
[3] A. Printz, S. Savagatrup, D. Burke, T. Purdy, D. Lipomi, Increased elasticity of a low-bandgap conjugated copolymer by random segmentation for mechanically robust solar cells, RSC Adv. 4 (2014) 13635, doi:http://dx.doi.org/10.1039/c4ra00029c.
[4] D. Tahk, H.H. Lee, D.-Y. Khang, Elastic moduli of organic electronic materials by the buckling method, Macromolecules 42 (2009) 7079, doi:http://dx.doi.org/10.1021/ma900137k.
[5] O. Awartani, B.I. Lemanski, H.W. Ro, L.J. Richter, D.M. DeLongchamp, B.T. O'Connor, Correlating stiffness, ductility, and morphology of polymer: fullerene films for solar cell applications, Adv. Energy Mater. 3 (2013) 399, doi:http://dx.doi.org/10.1002/aenm.201200595.
[6] B. O'Connor, E.P. Chan, C. Chan, B.R. Conrad, L.J. Richter, R.J. Kline, et al., Correlations between mechanical and electrical properties of polythiophenes, ACS Nano 4 (2010) 7538, doi:http://dx.doi.org/10.1021/nn1018768.
[7] J. Moulton, P. Smith, Electrical and mechanical properties of oriented poly (3-alkylthiophenes): 2. Effect of side-chain length, Polymer 33 (1992) 2340, doi:http://dx.doi.org/10.1016/0032-3861(92)90525-2.
[8] H.K. Reimschuessel, On the glass transition temperature of comblike polymers: effects of side chain length and backbone chain structure, J. Polym. Sci. Polym. Chem. Ed. 17 (1979) 2447, doi:http://dx.doi.org/10.1002/pol.1979.170170817.
[9] A. Postema, K. Liou, F. Wudl, P. Smith, Highly oriented low-modulus materials from liquid-crystalline polymers: the ultimate penalty for solubilizing alkyl side chains, Macromolecules 23 (1990) 1842, doi:http://dx.doi.org/10.1021/ma00208a048.
[10] J.Y. Kim, C.D. Frisbie, Correlation of phase behavior and charge transport in conjugated polymer/fullerene blends, J. Phys. Chem. C 112 (2008) 17726, doi:http://dx.doi.org/10.1021/jp8061493.
[11] T.F. O'Connor, A.V. Zaretski, B.A. Shiravi, S. Savagatrup, A.D. Printz, M.I. Diaz, et al., Stretching and conformal bonding of organic solar cells to hemispherical surfaces, Energy Environ. Sci. 7 (2014) 370, doi:http://dx.doi.org/10.1039/c3ee42898b.
[12] S.T. Salammal, E. Mikayelyan, S. Grigorian, U. Pietsch, N. Koenen, U. Scherf, et al., Impact of thermal annealing on the semicrystalline nanomorphology of spin-coated thin films of regioregular poly(3-alkylthiophene)s as observed by high-resolution transmission electron microscopy and grazing incidence X-ray diffraction, Macromolecules 45 (2012) 5575, doi:http://dx.doi.org/10.1021/ma300906v.
[13] A. Zhao, G. Swinnen, J. Van Assche, D. Manca, B. Vanderzande, Phase diagram of P3HT/PCBM blends and its implication for the stability of morphology, J. Phys. Chem. B 113 (2009) 1587, doi:http://dx.doi.org/10.1021/jp804151a.
[14] C. Bruner, F. Novoa, S. Dupont, R. Dauskardt, Decohesion kinetics in polymer organic solar cells, ACS Appl. Mater. Interfaces (2014) , doi:http://dx.doi.org/10.1021/am506482q.
[15] C. Friedel, N. McNeill, Influence of alkyl side-chain length on the performance of poly(3-alkylthiophene)/polyfluorene all-polymer solar cells, Chem. Mater. 22 (2010) 3389, doi:http://dx.doi.org/10.1021/cm100189t.
[16] M. Heeney, W. Zhang, D.J. Crouch, M.L. Chabinyc, S. Gordeyev, R. Hamilton, et al., Regioregular poly(3-hexyl) selenophene: a low band gap organic hole

transporting polymer, Chem. Commun. 47 (2007) 5061, doi:http://dx.doi.org/10.1039/b712398a.
[17] A. Pingel, R.D. Zen, F.C. Abellon, L.D.A. Grozema, D. Siebbeles, Temperature resolved local and macroscopic charge carrier transport in thin P3HT layers, Adv. Funct. Mater. 20 (2010) 2286, doi:http://dx.doi.org/10.1002/adfm.200902273.
[18] G. Giri, E. Verploegen, S.C.B. Mannsfeld, S. Atahan-Evrenk, D.H. Kim, S.Y. Lee, et al., Tuning charge transport in solution-sheared organic semiconductors using lattice strain, Nature 480 (2011) 504, doi:http://dx.doi.org/10.1038/nature10683.
[19] C.J. Bettinger, Z. Bao, Organic thin-film transistors fabricated on resorbable biomaterial substrates, Adv. Mater. 22 (2010) 651, doi:http://dx.doi.org/10.1002/adma.200902322.
[20] K.A. Singh, T. Young, R.D. McCullough, T. Kowaiewski, L.M. Porter, Planarization of polymeric field-effect transistors: improvement of nanomorphology and enhancement of electrical performance, Adv. Funct. Mater. 20 (2010) 2216, doi:http://dx.doi.org/10.1002/adfm.201000346.
[21] W.M.H. Sachtler, G.J.H. Dorgelo, A.A. Holscher, The work function of gold, Surf. Sci. 5 (1966) 221, doi:http://dx.doi.org/10.1063/1.1754539.
[22] Y. Park, D. Kim, Y. Jang, J. Cho, M. Hwang, Effect of side chain length on molecular ordering and field-effect mobility in poly(3-alkylthiophene) transistors, Org. Electron. 7 (2006) 514–520, doi:http://dx.doi.org/10.1016/j.orgel.2006.07.007.
[23] S.A. Choulis, J. Nelson, Y. Kim, D. Poplavskyy, T. Kreouzis, J.R. Durrant, et al., Investigation of transport properties in polymer/fullerene blends using time-of-flight photocurrent measurements, Appl. Phys. Lett. 83 (2003) 3812, doi:http://dx.doi.org/10.1063/1.1624636.
[24] E.J. Melzer, V.D. Koop, P.W.M. Mihailetchi, Hole transport in poly(phenylene vinylene)/methanofullerene bulk-heterojunction solar cells, Adv. Funct. Mater. 14 (2004) 865, doi:http://dx.doi.org/10.1002/adfm.200305156.
[25] P. Beaujuge, J. Fréchet, Molecular design and ordering effects in π-functional materials for transistor and solar cell applications, J. Am. Chem. Soc. 133 (2011) 20009, doi:http://dx.doi.org/10.1021/ja2073643.
[26] D.J. Lipomi, H. Chong, M. Vosgueritchian, J. Mei, Z. Bao, Toward mechanically robust and intrinsically stretchable organic solar cells: evolution of photovoltaic properties with tensile strain, Sol. Energy Mater. Sol. Cells 107 (2012) 355–365, doi:http://dx.doi.org/10.1016/j.solmat.2012.07.013.
[27] S. Savagatrup, E. Chan, S.M. Renteria-Garcia, A.D. Printz, A.V. Zaretski, T.F. O'Connor, et al., Plasticization of PEDOT:PSS by common additives for mechanically robust organic solar cells and wearable sensors, Adv. Funct. Mater. 25 (2015) 427, doi:http://dx.doi.org/10.1002/adfm.201401758.
[28] M.L. Treat, Phase separation in bulk heterojunctions of semiconducting polymers and fullerenes for photovoltaics, Annu. Rev. Phys. Chem. 65 (2014) 59, doi:http://dx.doi.org/10.1146/annurev-physchem-040513-103712.
[29] C. Bruner, R. Dauskardt, Role of molecular weight on the mechanical device properties of organic polymer solar cells, Macromolecules 47 (2014) 1117, doi:http://dx.doi.org/10.1021/ma402215j.
[30] F.P.V. Koch, M. Heeney, P. Smith, Thermal and structural characteristics of oligo (3-hexylthiophene)s (3HT) n, $n = 4–36$, J. Am. Chem. Soc. 135 (2013) 13699, doi:http://dx.doi.org/10.1021/ja405792b.
[31] A.D. Printz, S. Savagatrup, D. Rodriquez, D.J. Lipomi, Role of molecular mixing on the stiffness of polymer:fullerene bulk heterojunction films, Sol. Energy Mater. Sol. Cells 134 (2015) 64, doi:http://dx.doi.org/10.1016/j.solmat.2014.11.030.